A peptide from the adenovirus fiber shaft forms amyloid-type fibrils

Mary Luckey[a], Jean-François Hernandez[b], Gérard Arlaud[b], V. Trevor Forsyth[c], Rob W.H. Ruigrok[d], Anna Mitraki[b,*]

[a]*Department of Chemistry and Biochemistry, San Francisco State University, 1600 Holloway avenue, 94132 San Francisco, CA, USA*
[b]*Institut de Biologie Structurale, 41 rue Jules Horowitz, 38027 Grenoble Cedex 1, France*
[c]*Physics Department, Keele University, Staffordshire ST5 5BG, UK*
[d]*European Molecular Biology Laboratory, Grenoble Outstation, c/o Institut Laue-Langevin, 6 rue Jules Horowitz, BP 156, 38042 Grenoble Cedex 9, France*

Received 12 October 1999; received in revised form 29 December 1999

Edited by Pierre Jolles

Abstract The fiber protein of adenovirus consists of a C-terminal globular head, a shaft and a short N-terminal tail. The crystal structure of a stable domain comprising the head plus a part of the shaft of human adenovirus type 2 fiber has recently been solved at 2.4 Å resolution [van Raaij et al. (1999) Nature 401, 935–938]. A peptide corresponding to the portion of the shaft immediately adjacent to the head (residues 355–396) has been synthesized chemically. The peptide failed to assemble correctly and instead formed amyloid-type fibrils as assessed by electron microscopy, Congo red binding and X-ray diffraction. Peptides corresponding to the fiber shaft could provide a model system to study mechanisms of amyloid fibril formation.

Key words: Adenovirus; Amyloid fibril; Electron microscopy; Congo red; X-ray diffraction

1. Introduction

Numerous diseases such as Alzheimer's disease, maturity onset diabetes and transmissible spongiform encephalopathies are associated with deposition of insoluble fibrils named amyloid fibrils in tissues [2]. Current models of amyloid fibrils propose that the fibrils adopt a cross-β-structure with β-strands perpendicular to the fiber axis [3,4]. This cross-β-structure seems to be a structural motif common to all amyloid fibrils independent of sequence or structural folds of the proteins the fibrils originate from [4]. There is also a growing consensus that amyloid fibrils can evolve from common precursors, i.e. partially folded intermediates in the unfolding or refolding pathway of proteins [5–8]. Aggregate formation from partially folded intermediates that fail to proceed down to the correct folding pathway is also a common mechanism underlying inclusion body formation in laboratory and industry [9–14]. Despite a growing body of studies, the factors that govern the partition of polypeptide chains between correct folding and assembly on the one hand and misfolding and misassembly on the other remain poorly understood.

In the particular case of fibrillar proteins, for example collagen, correct chain assembly needs a registration signal. During collagen biosynthesis, the pro-collagen globular regions serve to properly align the three chains and are subsequently cleaved to give the mature, triple helical chain [15,16]. When the mature collagen is heated in vitro, the three chains unwind; upon subsequent cooling, segments of the triple helix reform, either within the same chain or between different chains, but they are out of register. The result is the formation of an intermolecular network that leads to the gelatin gel [15].

One of the approaches in studying protein folding consists in using synthetic peptides as models. Synthetic peptides corresponding to collagen sequences have opened a new dimension in the understanding of its folding and also of misfolding and misassembly associated with collagen diseases [17]. A model peptide that forms polymers that share at least some of the properties of the amyloid fibrils is the subject of this report. The peptide originates from a sequence of the adenovirus fiber protein. This trimeric protein is the cell attachment molecule of the virus, and consists of a globular head or knob, a shaft, and a short N-terminal tail anchored in the virus capsid [18,19]. The sequence of the shaft reveals pseudorepeats of 15 amino acids containing conserved hydrophobic residues and a conserved proline or glycine (Fig. 1A) [20]. The fiber of human adenovirus type 2 (HAd2) has 22 such repeats making up a total length of the shaft of 29 nm [21]. Recent folding studies have identified a stable domain of the fiber comprising the head plus five shaft repeats [22]. The crystal structure of this stable domain has just been solved at 2.4 Å resolution [1]. Each head monomer is an eight-stranded antiparallel β-sandwich, and the three monomers assemble into a three-bladed β-propeller structure [23,24]. The crystal structure reveals a novel folding motif for the shaft domain, named the triple β-spiral [1]. The structure of each repeat comprises an extended strand, then a type II β-turn which is followed by another β-strand. The repeats are connected to each other by a solvent-exposed variable loop (Fig. 1B). The hydrophobic residues are buried in the longitudinal hydrophobic core of the shaft or in a second ring of stabilizing hydrophobic interactions at a higher radius [1].

To study the folding of the shaft, we have synthesized a model peptide corresponding to the C-terminal part of the shaft in the stable domain. Hong and Engler reported in [25] that deletion of the first 354 residues of the HAd2 fiber did not prevent trimerization of the head and of the remaining portion of the shaft when the fragment was expressed in vaccinia cells. Therefore, that portion of the shaft (from residues

*Corresponding author. Fax: (33)-4-76 88 54 94.
E-mail: mitraki@ibs.fr

Abbreviations: Boc, *tert*-butyloxycarbonyl; HPLC, high performance liquid chromatography; GdnHCl, guanidine hydrochloride; HAd2, human adenovirus serotype 2; SDS, sodium dodecyl sulfate

PII: S0014-5793(00)01184-4

355 to 396, the beginning of the head) was chosen for the sequence of the synthetic peptide.

2. Materials and methods

2.1. Chemical reagents

tert-Butyloxycarbonyl (Boc) amino acids and resin were purchased from Neosystem (Strasbourg, France) or Novabiochem (Meudon, France). The reagents for solid-phase peptide synthesis were obtained from Applied Biosystems (Perkin Elmer, Courtaboeuf, France), except dichloromethane, which was from SDS (Solvants, Documentation, Synthèses) (Peypin, France), as was acetonitrile for high performance liquid chromatography (HPLC). 8 M Ultrapure guanidine hydrochloride (GdnHCl) was purchased from Pierce and Congo red was purchased from Sigma. All other chemicals were of the purest grade available.

2.2. Solid-phase peptide synthesis

The C-terminal amide derivative of the 355–396 segment from the HAd2 fiber protein was synthesized by the stepwise solid-phase method [26] using an Applied Biosystems 430A automated synthesizer. Synthesis was performed on a 4-methyl benzhydrylamine resin, and the Boc group was used for α-amino protection. All couplings were performed by the dicyclohexylcarbodiimide/1-hydroxybenzotriazole method, using *N*-methylpyrrolidone and dimethylsulfoxide as coupling solvents, according to the protocol defined by Applied Biosystems. Cleavage of the peptide from the resin and simultaneous deprotection of side chains were carried out in an HF cleavage apparatus (Peptide Institute, Japan) using liquefied HF in the presence of anisole and dimethylsulfide as scavengers for 1 h at −5°C.

The peptide was purified by reverse-phase HPLC on a Vydac (Hesperia, USA) C18 column (2.2×25 cm) by means of a linear gradient of 10–65% acetonitrile in 0.1% aqueous trifluoroacetic acid over 30 min (flow rate 16 ml/min). Homogeneous fractions were pooled and freeze-dried. The pronounced tendency of the peptide to aggregate during the purification steps hampered considerably the purification process and resulted in a low final yield of the material. The purity and identity of the synthetic peptide were assessed by reverse-phase HPLC and electrospray mass spectrometry [27]. The experimental mass was 4309.63 ± 0.2 (calculated mass 4309.83).

2.3. Electron microscopy

The peptide in 6 M GdnHCl at a concentration of 10 mg/ml was diluted to 0.4 mg/ml or 0.1 mg/ml with a pH 7 phosphate buffer (50 mM sodium phosphate, 1 mM EDTA). Alternatively, the peptide in 6 M GdnHCl was diluted to 0.1 mg/ml with a pH 4 acetate buffer (50 mM sodium acetate, 1 mM EDTA) or dissolved directly into pH 4 acetate buffer to the same final concentration. The peptide solution was adsorbed to the clean side of a carbon film on mica, washed with buffer without GdnHCl and negatively stained with 1% sodium silicotungstate. Micrographs were taken with a JEOL 1200 XII microscope and the magnification was calibrated with negatively stained crystals of catalase.

2.4. Congo red staining and polarized light microscopy

Fibrils were stained with 10 μM Congo red and were sedimented at 10 000×*g*. They were subsequently washed twice with phosphate buffer and then placed on glass slides. The samples were studied with a Zeiss Axiophot microscope equipped with crossed polars.

2.5. X-ray diffraction

To obtain the X-ray diffraction pattern, a peptide lacking the N-terminal asparagine residue (355) was used. This peptide could be obtained in higher yields but otherwise presents the same behavior in terms of aggregate formation, electron microscopy appearance and Congo red staining as the original peptide. Samples were prepared by dissolving the peptide (10 mg/ml concentration) in acetate buffer and forming droplets between the ends of two glass rods. The distance between the glass rods was gradually increased to encourage alignment of the fibrils while drying. The droplets were dried over a period of approximately 12 h, forming samples that were typically about 100–200 μm thick and 1–2 mm long.

X-ray diffraction patterns were recorded using a Siemens rotating anode generator that provided X-rays with a wavelength of 1.5418 Å. The detector was a Mar Research online image plate system. Exposure times ranged between 4 and 8 h.

3. Results and discussion

The synthetic peptide has a calculated p*I* of 8.4 at neutral pH; 12 out of its 42 residues are hydrophobic and seven are glycine. The purified peptide proved to be insoluble in buffer at neutral pH (50 mM sodium phosphate with 1 mM EDTA, pH 7) at a concentration of 10 mg/ml. In contrast, it was soluble in 6 M GdnHCl at the same concentration. When dissolved in 6 M GdnHCl and subsequently diluted to a concentration of 0.1 or 0.4 mg/ml with phosphate buffer, it formed fibrils. Fibrils were also formed when the peptide

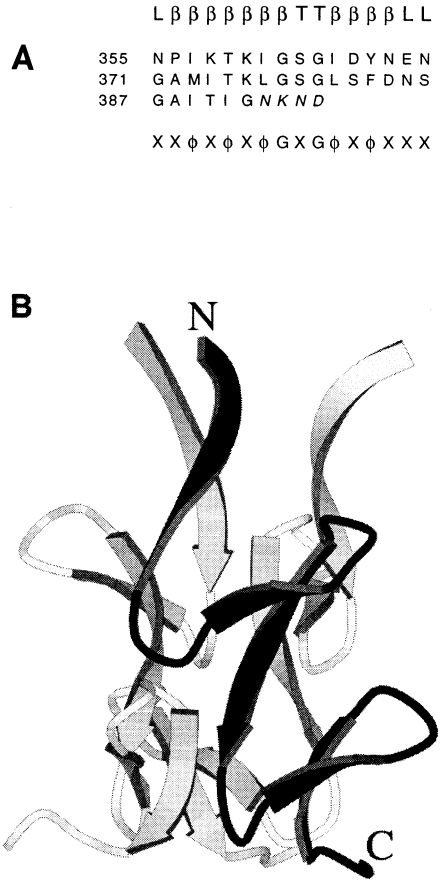

Fig. 1. Sequence of the synthetic shaft peptide 355–396 and structure of the corresponding segment within the native HAd2 fiber. (A) Sequence of the peptide of the HAd2 fiber shaft showing the approximately 15 residue repeats from residue 355 to 392. The last four amino acids are in italics and are not part of a repeat but connect the shaft to the head of the HAd2 fiber. The conserved secondary structure of the repeats is shown above the sequence with L for loop, β for β-strand and T for β-turn. The conserved sequence characteristics of the repeats are shown below the sequence with X for any residue, φ for hydrophobic residues and G for glycine. For the sequence of the fiber stable domain, see [22]. (B) Structure of the peptide within the native shaft segment (courtesy of Drs. Mark van Raaij and Stephen Cusack, EMBL Grenoble). One of the strands of the trimeric shaft is shown in black and the other two in gray. The structure of the peptide in the native shaft from N- to C-terminus consists of a β-strand, a type II β-turn, another β-strand and a surface-exposed loop leading to a second repeat with the same structure. The peptide ends with a relatively short β-strand plus four residues in random coil connecting the shaft to the head of the fiber.

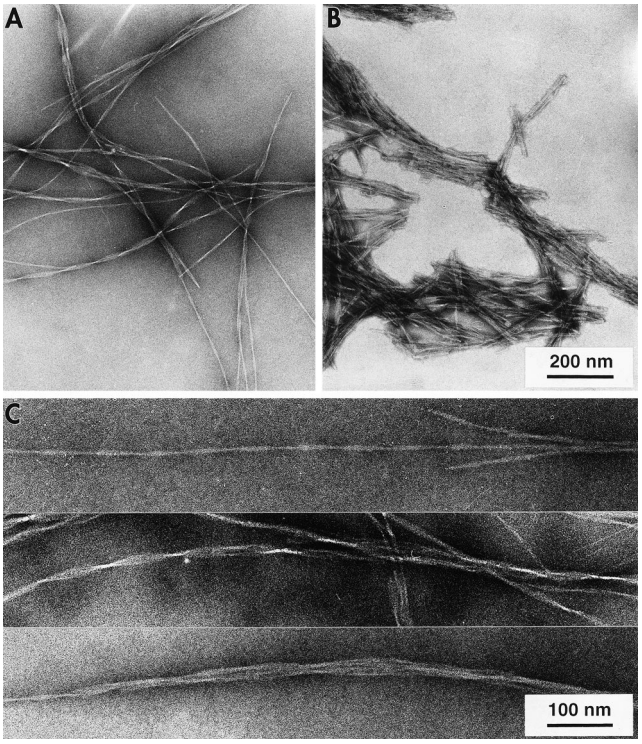

Fig. 2. Electron microscopy of fibrils. Electron micrographs of fibrils negatively stained with sodium silicotungstate. (A) Fibrils formed after dilution of peptide in 6 M GdnHCl into pH 7 buffer to a final concentration of 0.1 mg/ml. (B) Fibrils formed in the same way but after dilution to 0.4 mg/ml. (C) Higher magnification images of fibrils taken from the same sample as in A. Note the helical repeat structure. The magnification of A and B is the same, as indicated by the bar in B. The magnification of C is two times higher than that in A and B, as indicated by the bar in C.

was directly dissolved into 50 mM acetate buffer, 1 mM EDTA, pH 4, as well as when the peptide was first dissolved in 6 M GdnHCl and subsequently diluted into acetate buffer. Fibril formation could be detected by light scattering, following the UV absorbance at 340 nm or by right-angle scattering at 400 nm in a fluorimeter. In contrast with the stable domain of the native adenovirus fiber shaft, which is resistant to sodium dodecyl sulfate (SDS) [22], the fibril structure was not resistant to this detergent since it ran as monomers on SDS–polyacrylamide gel electrophoresis gels with or without prior heat treatment (not shown).

Electron microscopy of the freeze-dried peptide suspended in pH 7 buffer showed very large, unstructured aggregates, in agreement with the fact that the peptide is not soluble under these conditions. In contrast, the peptide solubilized in 6 M GdnHCl and subsequently diluted into pH 7 buffer to a final concentration of 0.4 mg/ml showed thin filaments with a length of 200–500 nm that had a strong tendency to coalesce and form large tangles (Fig. 2B). Samples that were diluted out of GdnHCl to a final concentration of 0.1 mg/ml revealed much longer unbranching strands that resemble twisted ribbons (Fig. 2A). Very similar filaments were observed after dilution to both pH 7 and pH 4 and also after direct dissolving in pH 4 buffer, indicating that the length of the filaments is mainly influenced by the peptide concentration at which they are formed. Higher magnification of a number of filaments is shown in Fig. 2C. These images seem to provide support for the occurrence of thin protofilaments that associate sideways to form twisted ribbons with variable widths, depending on how many protofilaments are present. The thickness of the nodules of all ribbons was the same: 3.7 ± 0.5 nm ($n = 18$). The distance between the nodules, i.e. half of the helical pitch, was 84 ± 11 nm ($n = 47$). Similar twisted ribbons have been observed in amyloid fibrils formed by fusion peptides (thickness about 5 nm, half pitch of about 100 nm; [28]), an SH3 domain (half pitch 54–66 nm; [29]) and various Alzheimer's disease-related peptides (thicknesses of 3.5–4 nm to 5.5–6 nm; [30]).

When Congo red was added to the fibril-forming peptide solutions, the absorption spectrum of the dye was broad with a maximum at 506 nm, compared to an absorption spectrum with a maximum at 492 nm of the dye alone in buffer. Visible red fibrils were observed at the bottom of the test tube. To view the fibrils under a light microscope, the sample needed to be concentrated in a microfuge; as a result, the fibrils were found to coalesce into plaques (Fig. 3A). When viewed under polarized light, these plaques exhibited birefringence, going from red to green (Fig. 3B).

The X-ray diffraction pattern of the fibrils showed two major reflections that appear as rings due to the poor alignment of the fibrils. A dominant sharp reflection was observed at a position corresponding to 4.75 Å and a weaker, more diffuse one was observed at 9.7 Å (Fig. 4). Those reflections are characteristic of the cross-β-conformation described for numerous amyloid fibrils, where β-sheets run parallel to the filament axis with their constituent β-strands being perpendicular to the main fibril axis [31]. In well-oriented amyloid fibril samples, the 4.75 Å reflection is meridional in character and

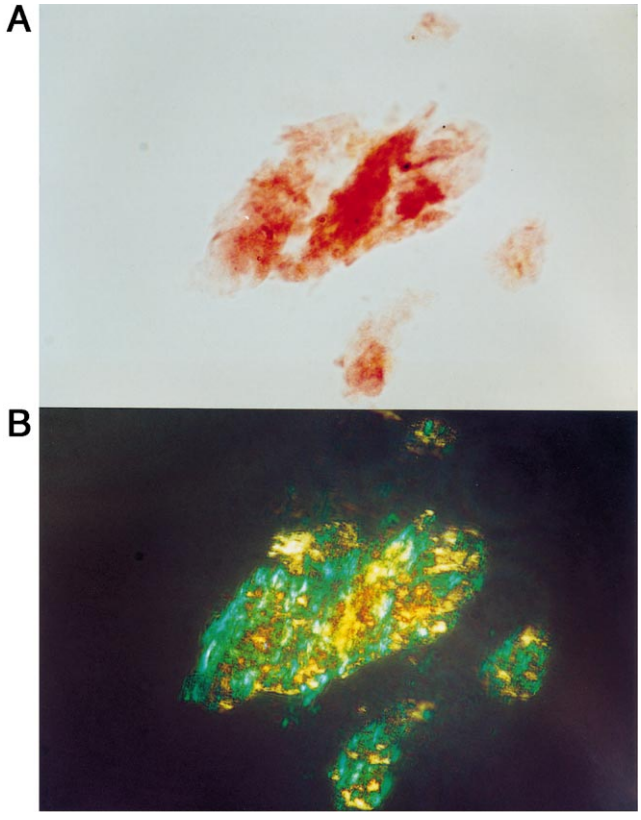

Fig. 3. Photomicrographs of peptide fibrils stained with Congo red. (A) Bright field, (B) polarized light. Magnification is 100×.

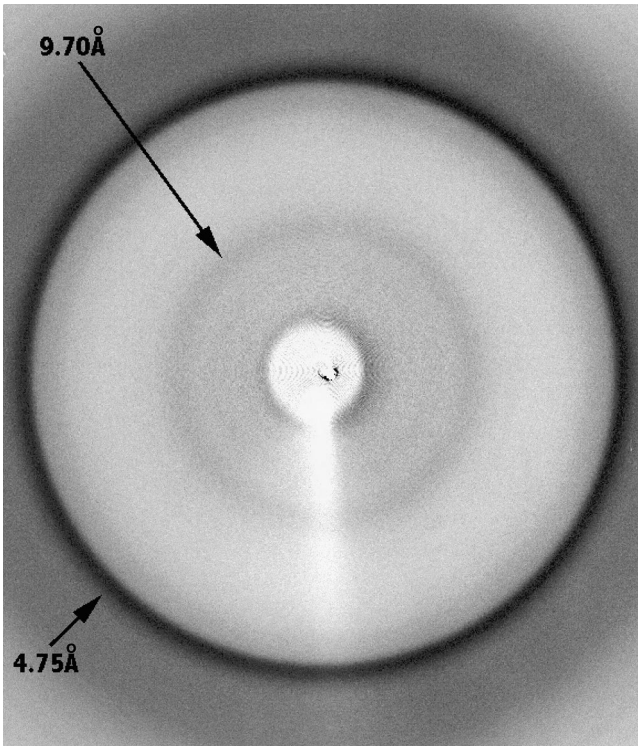

Fig. 4. X-ray diffraction pattern of the fibrils. Two major reflections characteristic of the amyloid fibrils (4.75 and 9.7 Å) are marked by arrows. Due to the poor alignment of fibrils, those reflections appear as rings.

corresponds to the interstrand spacing in the cross-β-conformation, while the 9.7 Å one is equatorial and corresponds to the intersheet spacing. Although the method of sample preparation that was used is designed to produce aligned samples in which the filaments are expected to be predominantly parallel, none of the diffraction patterns that have been obtained so far has shown good orientation. Attempts to improve the ordering in these fibers are currently in progress so that a detailed fiber diffraction analysis can be undertaken.

These results show that the HAd2 model peptide studied is capable of forming fibrils that share common characteristics with well-characterized amyloid fibrils, namely the ability to form insoluble strands of indeterminate length that are birefringent when stained with Congo red and display two characteristic major reflections in X-ray diffraction patterns. The conformation of the peptide within the fibrils is probably different from the one within the native adenovirus fiber shaft. It is possible that the peptide adopts a partially folded conformation [32] that could subsequently convert to the cross-β-conformation described for numerous amyloid structures [31,33].

The adenovirus fiber head is known to be essential for its trimerization as deletions or mutations in this part of the protein hinder the trimerization process in vivo [25,34]. The fiber head might act as a registration signal necessary for the three chains to align and fold together, thus playing a role analogous to that of the pro-collagen peptides in collagen folding [15,16,35]. A plausible model to explain fibril formation would be that in the absence of the head to establish registration, oligomers can form through out of register interactions leading to long unbranched sub-protofilaments. These sub-protofilaments could then associate into protofilaments as proposed for amyloid fibrils formed from other proteins or peptides [3,4].

In order to address these questions, it will be necessary to obtain higher resolution structural information on fibril architecture, especially using X-ray diffraction and cryo-electron microscopy. It will also be interesting to study the folding and polymerization behavior of other peptides derived from the HAd2 fiber shaft, with different lengths and overall charges. We anticipate that these peptides can serve as model systems for the further understanding of the interplay between assembly and misassembly processes in β-sheet structures.

Acknowledgements: We thank Yves Usson of the Institut Albert-Bonniot, Grenoble, France, for help with the use of the polarized light microscope and Yves Pétillot for mass spectroscopy. We are grateful to Dr. Mark van Raaij of EMBL Grenoble for providing Fig. 1B. This work was supported in part by the CEA (Commissariat à l'Energie Atomique) and the CNRS (Centre National de la Recherche Scientifique). M.L. acknowledges financial support from the CEA during a sabbatical stay in Grenoble. This is publication no. 730 from the Institut de Biologie Structurale.

References

[1] van Raaij, M.J., Mitraki, A., Lavigne, G. and Cusack, S. (1999) Nature 401, 935–938.
[2] Sipe, J.D. (1992) Ann. Rev. Biochem. 61, 947–975.
[3] Blake, C. and Serpell, L. (1996) Structure 4, 989–998.
[4] Sunde, M., Serpell, L.C., Bartlam, M., Fraser, P.E., Pepys, M.B. and Blake, C.C. (1997) J. Mol. Biol. 273, 729–739.
[5] Kelly, J.W. (1996) Curr. Opin. Struct. Biol. 6, 11–17.
[6] Kelly, J.W. (1997) Structure 5, 595–600.
[7] Wetzel, R. (1996) Cell 86, 699–702.
[8] Guijarro, J.I., Sunde, M., Jones, J.A., Campbell, I.D. and Dobson, C.M. (1998) Proc. Natl. Acad. Sci. USA 95, 4224–4228.
[9] Mitraki, A. and King, J. (1989) Bio/Technology 7, 690–699.
[10] Wetzel, R. (1994) Trends Biotechnol. 12, 193–198.
[11] King, J., Haase-Pettingell, C., Robinson, A.S., Speed, M. and Mitraki, A. (1996) FASEB J. 10, 57–66.
[12] Fink, A.L. (1998) Fold. Des. 3, R9–R23.
[13] Jaenicke, R. and Seckler, R. (1997) Adv. Protein Chem. 50, 1–59.
[14] Betts, S. and King, J. (1999) Struct. Fold. Des. 7, R131–R139.
[15] Engel, J. and Prockop, D.J. (1991) Ann. Rev. Biophys. Biophys. Chem. 20, 137–152.
[16] McLaughlin, S.H. and Bulleid, N.J. (1998) Matrix Biol. 16, 369–377.
[17] Baum, J. and Brodsky, B. (1999) Curr. Opin. Struct. Biol. 9, 122–128.
[18] Devaux, C., Caillet-Boudin, M.L., Jacrot, B. and Boulanger, P. (1987) Virology 161, 121–128.
[19] Chroboczek, J., Ruigrok, R.W. and Cusack, S. (1995) Curr. Top. Microbiol. Immunol. 199, 163–200.
[20] Green, N.M., Wrigley, N.G., Russell, W.C., Martin, S.R. and McLachlan, A.D. (1983) EMBO J. 2, 1357–1365.
[21] Ruigrok, R.W., Barge, A., Albiges-Rizo, C. and Dayan, S. (1990) J. Mol. Biol. 215, 589–596.
[22] Mitraki, A., Barge, A., Chroboczek, J., Andrieu, J.P., Gagnon, J. and Ruigrok, R.W. (1999) Eur. J. Biochem. 264, 599–606.
[23] Xia, D., Henry, L.J., Gerard, R.D. and Deisenhofer, J. (1994) Structure 2, 1259–1270.
[24] van Raaij, M.J., Louis, N., Chroboczeck, J. and Cusack, S. (1999) Virology 262, 333–343.
[25] Hong, J.S. and Engler, J.A. (1996) J. Virol. 70, 7071–7078.
[26] Barany, G. and Merrifield, R.B. (1980) The Peptides 2 (Gross, E. and Meienhofer, J., Eds.), pp. 1–284, Academic Press, New York.
[27] Pétillot, Y., Thibault, P., Thielens, N.M., Rossi, V., Lacroix, M., Coddeville, B., Spik, G., Schumaker, V.N., Gagnon, J. and Arlaud, G.J. (1995) FEBS Lett. 358, 323–328.
[28] Ulrich, A.S., Tichelaar, W., Forster, G., Zschornig, O., Weinkauf, S. and Meyer, H.W. (1999) Biophys. J. 77, 829–841.

[29] Jimenez, J.L., Guijarro, J.I., Orlova, E., Zurdo, J., Dobson, C.M., Sunde, M. and Saibil, H.R. (1999) EMBO J. 18, 815–821.
[30] Fraser, P.E., Nguyen, J.T., Surewicz, W.K. and Kirschner, D.A. (1991) Biophys. J. 60, 1190–1201.
[31] Sunde, M. and Blake, C. (1997) Adv. Prot. Chem. 50, 123–159.
[32] Kayed, R., Bernhagen, J., Greenfield, N., Sweimeh, K., Brunner, H., Voelter, W. and Kapurniotu, A. (1999) J. Mol. Biol. 287, 781–796.
[33] Dobson, C.M. (1999) Trends Biochem. Sci. 24, 329–332.
[34] Novelli, A. and Boulanger, P.A. (1991) Virology 185, 365–376.
[35] van der Rest, M., Dublet, B., Labourdette, L. and Ricard-Blum, S. (1999) Proc. Indian Acad. Sci. (Chem. Sci.) 111, 105–113.